Inlet and outlet characteristics boundary conditions for large eddy simulations of turbomachinery

Nicolas Odier, Thierry Poinsot, Florent Duchaine, Laurent Gicquel, Stéphane Moreau

INLET AND OUTLET CHARACTERISTICS BOUNDARY CONDITIONS FOR LARGE EDDY SIMULATIONS OF TURBOMACHINERY

Nicolas Odier,
Thierry Poinsot, Florent Duchaine,
Laurent Gicquel
CFD Team
CERFACS
31057 Toulouse, France
Email: nicolas.odier@cerfacs.fr

Stéphane Moreau

University of Sherbrooke
Sherbrooke,
QC J1K 2R1, Canada

ABSTRACT

Inlet an outlet boundary conditions are essential elements of any CFD predictions and this is even more so for turbomachinery Large Eddy Simulations, either applied to academic or industrial configurations. For compressible solvers, non-reflecting, characteristic inlet boundary condition imposing total pressure, total temperature and flow direction is usually needed, while an outlet relaxation methodology that automatically adapts the outlet static pressure as a function of the desired mass-flow rate rate is used for turbomachinery flow predictions. Establishing such a framework is clearly desirable especially for industrial use of LES. Development and validations remain necessary in such a fully unsteady context as detailled hereafter.

INTRODUCTION

Available computational ressources have enabled since a few decades a growing litterature in the field of unsteady numerical simulations for complex geometries. With this gain of ressources, Large-Eddy Simulation (LES) is becoming a performant tool to predict losses (Scillitoe et *al*., [1], Legget et *al*. [2]), acoustic (Pogorelov et *al*. [3], Tyacke et *al*. [4], Salas and Moreau [5]), or wall heat transfer (Collado Morata [6]), that are key topics on which industrials need to focus on to increase efficiency and reduce the emitted noise of next generation of engines. Some comprehensive reviews of LES for turbomachinery may be found in Dufour et *al*. [7], Gourdain et *al*. [8], Tucker et *al*. [9–11]. When considering Large Eddy Simulation and Direct Numerical Simulation (DNS) in a compressor or turbine stage, several points are to be cautiously addressed: among others, mesh and numerical scheme need to be accurate enough to ensure proper initiation and advection of turbulent structure with as little dissipation and dispersion as possible. Wall-treatment must also be taken into account depending on the final application. Depending on the available computational ressource, wall-resolved LES may help transition of the boundary layer or wall heat transfer prediction in academic cases (Segui et *al*. [12], Sayadi and Moin [13]), but remains too expensive for real configurations where hybrid methodologies are to be considered. In this case, many hybrid RANS-LES methodologies have been proposed: Detached-Eddy Simulations (Spalart et *al*. [14]), Zonal DES (Deck [15]) or Zonal LES (Boudet et *al*. [16]), Wall-modeled LES (Bose and Park [17]). To finish, a last crucial point that is often disregarded in favour to the previous points is to impose acoustically non-reflecting inlet and outlet boundary conditions as well as turbulence injection. A usual way to prescribe the inlet boundary condition for turbomachinery applications is the imposition of a total pressure, total temperature, and flow angle. However, imposing such a piece of information while remaining acoustically non reflecting is rarely detailed. Likewise, the outlet

boundary condition usually specifies a static pressure, that must comply with the establishement of a radial equilibrium. Finally, this outlet static pressure must be enforced so that the desired mass-flow rate is established within the turbomachinery, given the inlet total pressure and temperature. Determining this outlet static pressure is not an easy task since it is rarely known in advance, and depends on the general work and losses occuring in the considered configuration. Current academic use of LES usually involves iterative procedures to specify these parameters, but with the growing use of unsteady simulations expected in an industrial context (Larsson and Wang [18], Gourdain et *al*. [8]), such a strategy will no more be acceptable.

This specific issue of inlet and outlet boundary condition specification for LES of turbomachinery configurations in an industrial context is addressed in this paper. After a description of the numerical methodology in the second section, the characteristic formulation required for an inlet turbomachinery condition is presented in the third section, based on Odier et *al*. [19]. Finally, a relaxation methodology to automatically prescribe the outlet static pressure is proposed in the fourth section, prior to a set of validation test-cases.

NUMERICAL SOLVER

The present study is performed using an unsteady compressible unstructured and massively parallel solver, AVBP, detailed in Schønfeld et *al*. [20] and Gourdain et *al*. [21]. This solver, initially devoted to combustion applications, relies on an explicit Lax-Wendroff [22] 2nd order accurate in space and time numerical scheme, or a TTG4A 3rd order in space, 4th-order in time numerical scheme (Colin and Rudgyard, [23]). To deal with rotor-stator interface in this unsteady context, the MISCOG (Multi Instance Solver Coupled through Overlapping Grids) methodology is considered. This methodology, detailed in Wang et *al*. [24], consists in coupling two LES computations – one for the static domain, the other for the rotating part –, through the use of an overset grid method. This methodology has proven its ability to ensure a 3rd-order in space numerical scheme trough the interface (De Laborderie et *al*. [25]), and has been applied to various turbomachinery configurations: multistage or centrifugal compressor (De Laborderie et *al*. [26], Dombard et *al*. [27], Wang et *al*. [28]), fans (Leonard et *al*. [29], Odier et *al*. [30], Perez-Arroyo et *al*. [31]), combustor-turbine configuration (Duchaine et *al*. [32], turbine stage (Papadogiannis et *al*. [33]), Wang et *al*. [34]).

INLET CONDITION: P_t, T_t AND FLOW DIRECTION PRESCRIPTION

Formulation

As recalled in the introduction, a methodology able to prescribe the inlet target values without acoustic reflection must be considered for an unsteady compressible turbomachinery simulation. The characteristic methodology first described by Thompson [35] for Euler equations and then extended to Navier-Stokes equations by Poinsot and Lele [36] is followed here to address this issue. In this case, the methodology consists in rewriting the Navier-Stokes primitives variables in term of 1D characteristics waves, following Eqs. (1):

$$\begin{pmatrix} \mathscr{L}_+ \\ \mathscr{L}_- \\ \mathscr{L}_{t_1} \\ \mathscr{L}_{t_2} \\ \mathscr{L}_S \end{pmatrix} = \begin{pmatrix} (u_n+c)\left(\frac{\partial u_n}{\partial n}+\frac{1}{\rho c}\frac{\partial P_s}{\partial n}\right) \\ (u_n-c)\left(-\frac{\partial u_n}{\partial n}+\frac{1}{\rho c}\frac{\partial P_s}{\partial n}\right) \\ u_n\frac{\partial u_{t_1}}{\partial n} \\ u_n\frac{\partial u_{t_2}}{\partial n} \\ u_n\left(\frac{\partial \rho}{\partial n}-\frac{1}{c^2}\frac{\partial P_s}{\partial n}\right) \end{pmatrix} \tag{1}$$

where n stands for the normal direction to the boundary surface. For a subsonic inlet, $\mathscr{L}_+$ $\mathscr{L}_{t_1}$, $\mathscr{L}_{t_2}$ and $\mathscr{L}_S$ are respectively the ingoing acoustic wave, the two shear waves, and the entropic wave that have to be determined, while $\mathscr{L}_-$, the outgoing acoustic wave, is known from the computational domain. Poinsot and Lele [36] proposed to consider a locally one-dimensional inviscid flow (LODI) to determine the unknown wave amplitudes depending on the desired condition. In this original work, the wave amplitudes are related to account for the imposition of a velocity magnitude, its direction, static pressure and species composition at the inlet. However, wave relations to impose total pressure $P_t = P_s\left(1+\frac{\gamma-1}{2}M^2\right)^{\left(\frac{\gamma}{\gamma-1}\right)}$, total temperature $T_t = T_s\left(1+\frac{\gamma-1}{2}M^2\right)$, flow direction, and species composition are not provided. Odier et *al*. [19] have recently proposed relations dedicated to impose P_t, T_t and flow direction. Among the different possible relations, the non-reflecting "**Pt-Tt-NSCBC-NR**" boundary condition is of specific interest for turbomachinery applications. For this condition, derived for a constant adiabatic coefficient γ, the waves are expressed as

$$\mathscr{L}_{t_1} = -\frac{\partial u_{t_1}}{\partial t} \tag{2}$$

$$\mathscr{L}_{t_2} = -\frac{\partial u_{t_2}}{\partial t} \tag{3}$$

$$\mathscr{L}_k = Y_k \mathscr{L}_S - \rho \frac{\partial Y_k}{\partial t} \tag{4}$$

$$\mathscr{L}_+ = \frac{F_1 \frac{\partial T_t}{\partial t} + F_2 \frac{\partial P_t}{\partial t} + \frac{P_t}{rT_t} \cdot F_2 F_3 + \frac{1}{C_p} \cdot F_1 F_3 + F_1 \cdot \frac{T_t}{r} \sum_{k=1}^{N} r_k \frac{\partial Y_k}{\partial t}}{F_4 F_2 + F_5 F_1} \tag{5}$$

$$\mathscr{L}_S = \frac{\frac{\partial T_t}{\partial t} + \frac{1}{C_p} F_3 + \frac{T_t}{r} \sum_{k=1}^{N} r_k \frac{\partial Y_k}{\partial t} - F_5 \cdot \mathscr{L}_+}{F_2} \tag{6}$$

where Y_k is the mass fraction of species k, and

$$F_1 = \frac{e_c}{\rho} \cdot \frac{P_t}{rT_t} \tag{7}$$

$$F_2 = \frac{T_t}{\rho} - \frac{e_c}{\rho C_p} \tag{8}$$

$$F_3 = \mathscr{L}_{t_1} u_{t_1} + \mathscr{L}_{t_2} u_{t_2} \tag{9}$$

$$F_4 = \left(-\frac{\rho c}{2} \cdot \frac{P_t}{P_s} + \frac{P_t}{rT_t} \cdot \left(\frac{(\gamma - 1) e_c}{2c} - \frac{u_n}{2} \right) \right) \tag{10}$$

$$F_5 = \left(-\frac{(\gamma - 1) T_t}{2c} + \frac{1}{C_p} \left(\frac{(\gamma - 1) e_c}{2c} - \frac{u_n}{2} \right) \right) \tag{11}$$

The inlet flow direction is then enforced through the prescription of $sin(\phi)$ and $sin(\theta)$ where ϕ and θ are the flow angles depicted in Fig. 1. This choice also enforces the two shear waves accordingly since,

$$\frac{\partial u_{t_1}}{\partial t} = \frac{\partial}{\partial t} \left(\| \overrightarrow{U} \| \times (sin(\theta)) \right) = -\mathscr{L}_{t_1} \tag{12}$$

$$\frac{\partial u_{t_2}}{\partial t} = \frac{\partial}{\partial t} \left(\| \overrightarrow{U} \| \times (sin(\phi)) \right) = -\mathscr{L}_{t_2} \tag{13}$$

in which $\| \overrightarrow{U} \| = \sqrt{{u_n}^2 + {u_{t_1}}^2 + {u_{t_2}}^2}$. Note that this velocity magnitude is not imposed by the methodology, only the angular components θ and ϕ are prescribed.

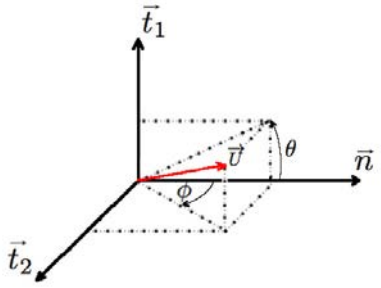

FIGURE 1: VELOCITY VECTOR $\overrightarrow{U}$, AND CORRESPONDING ANGLES θ AND ϕ.

A known issue of the LODI non-reflecting boundary condition is its property to "drift" from the target value of interest mainly because of the underlined hypotheses. To address this issue, Rudy and Strikwerda [37] introduced a linear relaxation method writing any quantity of interest temporal derivative $\frac{\partial X}{\partial t}$dt under the form:

$$\frac{\partial X}{\partial t} \mathrm{dt} = -\sigma_X \left(X_{predicted} - X_{target} \right) \tag{14}$$

where σ_X is a relaxation coefficient and comes as a complement to previous relations. In this present study, the relaxation coefficients for every X variables are chosen to be equals, so $\sigma_X = \sigma_{P_t} = \sigma_{T_t} = \sigma_{u_{t_1}} = \sigma_{u_{t_2}}$.

Convergence towards desired values

The convergence of the average quantities of interest towards the prescribed value at an inlet boundary condition is studied in this subsection for an academic test case, to illustrate the effect of the relaxation coefficient. The considered test-case is depicted in Fig. 2, and consists of an inlet boundary condition where total pressure and temperature are imposed, as well as a normal direction to the boundary surface. The outlet characteristic condition imposes a static pressure, and periodic conditions

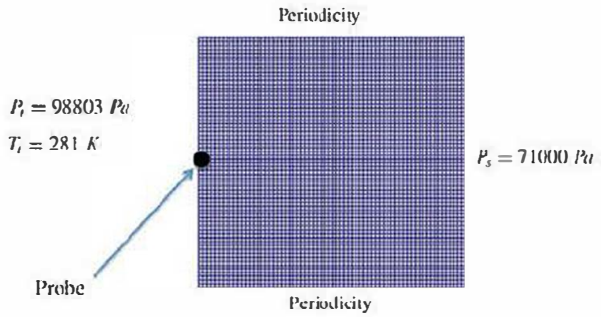

FIGURE 2: TEST CASE UNDER STUDY

on the top and bottom are applied. The outlet static pressure is chosen so that the resulting Mach number yields a compressible flow. For $\gamma = 1.4$ and $P_s = 71000$ Pa, the resulting Mach number is given by Eq. (15):

$$M = \sqrt{\frac{2}{\gamma - 1}\left(\left(\frac{P_t}{P_s}\right)^{\frac{\gamma-1}{\gamma}} - 1\right)} = 0.7036 \qquad (15)$$

An arbitrary initial solution is chosen, consisting of a uniform static pressure $P_s = 98803$ Pa, a uniform static temperature $T_s = 281\ K$, and a uniform velocity field $U = 10\ m/s$.

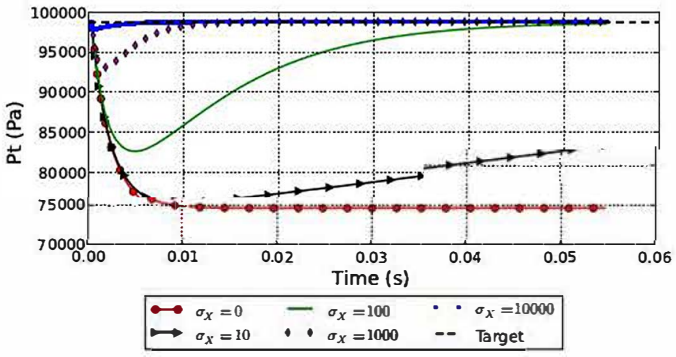

FIGURE 3: EVOLUTION OF THE INLET TOTAL PRESSURE P_t FOR DIFFERENT VALUES OF RELAXATION COEFFICIENTS σ_X

At the inflow, the temporal evolutions of P_t, T_t and of the Mach number M for different relaxation coefficients σ_X are reported in Figs. 3 to 5 respectively. These results prove the

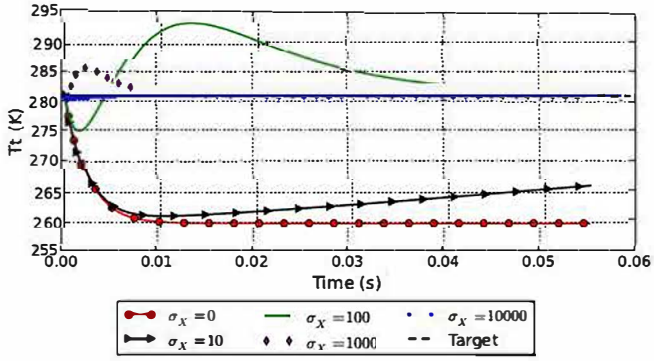

FIGURE 4: EVOLUTION OF THE INLET TOTAL TEMPERATURE T_t FOR DIFFERENT VALUES OF RELAXATION COEFFICIENTS σ_X

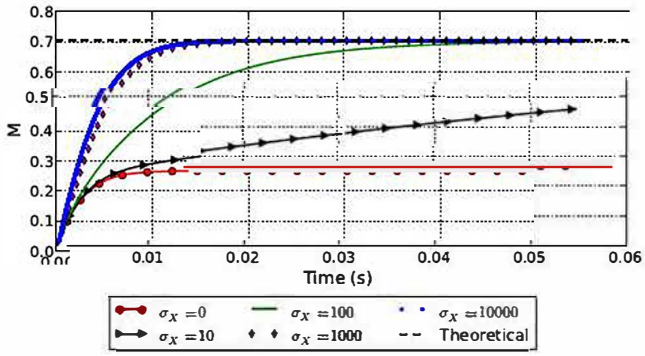

FIGURE 5: EVOLUTION OF THE INLET MACH NUMBER M FOR DIFFERENT VALUES OF RELAXATION COEFFICIENTS σ_X

convergence towards the prescribed values, as soon as the relaxation coefficients are not zero. Increasing the relaxation coefficients increases the convergence speed, but is also likely to increase the resulting acoustic reflectivity. Odier et *al.* [19] however showed that reflection remains small for the considered configuration. Enforcement of large relaxation coefficients is recommended only for the flow establishement. These σ_X values should then be reduced as much as possible as soon as the flow is established to ensure fully non-reflective inflow. The important message from these tests is that the unphysical establishement of the flow is a strong function of the inflow and initial guess which need to be carefully addressed for efficient CPU use of such simulations.

Turbulence injection

A brief insight of the coupling with turbulence injection is given in the present subsection. The proposed boundary condition may be coupled with a synthetic turbulence injection relying on random flow generation based on the methodologies proposed by Kraichan [38] then extended by Smirnov et *al*. [39] for non-homogeneous anisotropic fluctuations generation. The general idea consists in generating a fluctuating velocity field from a sample of random Fourier harmonics, thus considering the turbulent flow as a sum of N periodic Gaussian vortices, so shaped that a Passot-Pouquet [40] energy spectrum is reached in the limit $N \to \infty$. The three resulting unsteady velocity components (u'_1, u'_2, u'_3) are added to the inlet acoustic waves given in Eqs. (2), (3) and (5) governing the mean flow, so that:

$$\mathscr{L}_{+_{turb}} = \mathscr{L}_{+} + \frac{\partial u'_1}{\partial t} \tag{16}$$

$$\mathscr{L}_{t_{1_{turb}}} = \mathscr{L}_{t_1} + \frac{\partial u'_2}{\partial t} \tag{17}$$

$$\mathscr{L}_{t_{2_{turb}}} = \mathscr{L}_{t_2} + \frac{\partial u'_3}{\partial t} \tag{18}$$

This methodology follows the VFCBC formalism proposed by Guézennec and Poinsot [41] for a boundary imposing the velocity and the static temperature. The resulting turbulent characteristics, as well as the acoustic properties with such a turbulence injection are given in Odier et *al*. [19].

OUTLET BOUNDARY CONDITION: P_s RELAXATION TOWARD A DESIRED MASS-FLOW RATE

At a subsonic outlet boundary condition, the only wave to be prescribed is the entering acoustic one $\mathscr{L}_{-}$, since all other waves are known and come from the computational domain. A characteristic formulation imposing a static pressure is detailed in Poinsot and Lele [36], and reads:

$$\mathscr{L}_{-} = \frac{\partial P}{\partial t} \tag{19}$$

This formulation has been later improved by Lodato et *al*. [42] and Granet et *al*. [43] to account for transverse terms, to ensure vortice convection through the outlet boundary. Finally, Koupper et *al*. [44] have shown that this characteristic formalism is compatible with turbomachinery applications since the radial equilibrium is naturally satisfied.

In practical LES since a total pressure and temperature are specified at the inlet, the static pressure value at the outlet must be prescribed until the desired mass-flow rate is reached within the turbomachinery. Unfortunately, this pressure value is not known a-priori and depends on the overall pressure losses of the configuration, on the work given or received by the flow, and must be determined manually by the user in agreement with the outlet information. A growing use of LES in an industrial context might be expected in the next decade, to complement RANS predictions or 0D analytical models. This manual determination of the outlet static pressure is thus not satisfying in such a context, where several points of a characteristic line are to be simulated. First examples of characteristic line predictions in a complex industrial configuration using LES may be found in De Laborderie et *al*. [45] and Dombard et *al*. [27]. A dedicated relaxation methodology that allows an outlet static pressure adaptation is proposed in this section, as well as a best-practise guideline for its use.

Formulation

The proposed formulation consists in modifying the imposed outlet static pressure every T_{update} periods of time, depending on the average mass-flow rate evaluated during this time interval. This relaxation methodology can be expressed by:

$$P_{s_{corrected}} = \bar{P}_s + K(\bar{Q} - Q_{ref}) \tag{20}$$

where $P_{s_{corrected}}$ is the static pressure to be imposed at the outlet condition, $\bar{P}_s$ is the time-averaged static outlet pressure obtained by averaging the simulation over the duration T_{update}, K is a relaxation coefficient expressed in $m^{-1}s^{-1}$, while $\bar{Q}$ is the time-averaged mass-flow rate through the outlet condition provided by the simulation during T_{update}. To finish, Q_{ref} is the target mass-flow rate specified for this specific condition as defined by 0D evaluation for example.

Subsonic turbine-blade channel

The proposed methodology is tested on a linear cooled turbine cascade depicted in Fig. 6, part of the wind tunnel for linear cascade facility at DLR Göttingen (Aillaud et *al*. [46], Rehder [47, 48]). The mesh consists in 7 millions cells. The inlet condition is treated using the above characteristic formulation with imposed target values $P_t = 98000\ Pa$, $T_t = 293\ K$ and a flow direction to ensure a zero blade angle of attack. An arbitrary initial uniform solution is considered to start the simulation, with $P_s = 91140\ Pa$, $T_s = 287\ K$ in the whole domain, as well as a

zero velocity field. Since the experimental velocity fluctuation is lower that 1% (Redher [48]), no inlet turbulence is added.

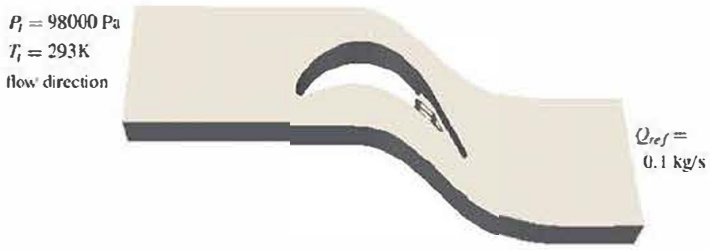

FIGURE 6: TURBINE BLADE CONFIGURATION.

A subsonic case is targeted in this subsection, with a desired mass-flow rate of $Q_{ref} = 0.1$ kg/s. The outlet pressure is updated every $T_{update} = 25.0 * 10^{-5}$ s which corresponds to 0.5 flow through blade passage about, and the relaxation coefficient is chosen to $K = 2.0 * 10^5\ (m.s)^{-1}$. The value of K was obtained after several tests, to find an appropriate value allowing both suffisant outlet pressure amplitude variations, without too large amplitude that would lead to instabilities. Note that the finding of an appropriate K value is the critical part of the proposed methodology.

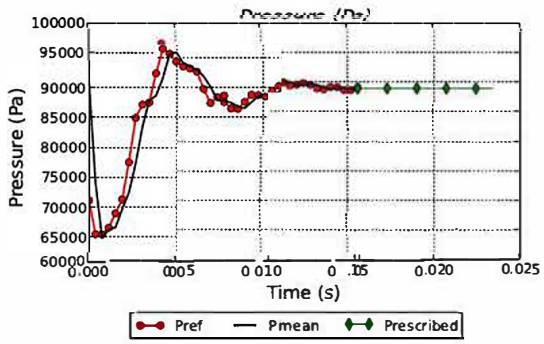

FIGURE 7: SUBSONIC TURBINE BLADE: OUTLET PRESSURE EVOLUTION.

The outlet static pressure evolution and the mass-flow rate through the outlet boundary temporal evolutions are shown in Fig. 7 and Fig. 8 respectively. Both the actual average pressure on the outlet boundary surface ($\bar{P}_s$ in Eq.(20)) and the prescribed

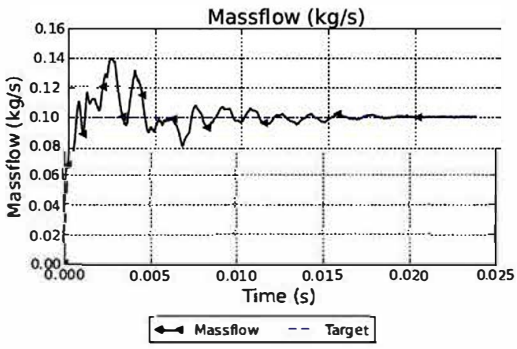

FIGURE 8: SUBSONIC TURBINE BLADE: OUTLET MASSFLOW EVOLUTION.

pressure ($P_{s_{corrected}}$ in Eq.(20)) are plotted in Fig. 7, showing that the actual mean pressure quickly follows the prescription and that these two pressures evolve towards $P_s = 88900$ Pa while the mass-flow rate converges toward $Q = Q_{ref}$. At time $t = 0.0155\ s$, the relaxation methodology is no longer considered and a fixed static pressure $P_s = 88900$ Pa is imposed at the outlet, in order to ensure that the desired mass-flow rate Q_{ref} has actually been reached without forcing the flow into an unphysical solution. The total computational cost is 5800 hCPU using 240 MPI processes.

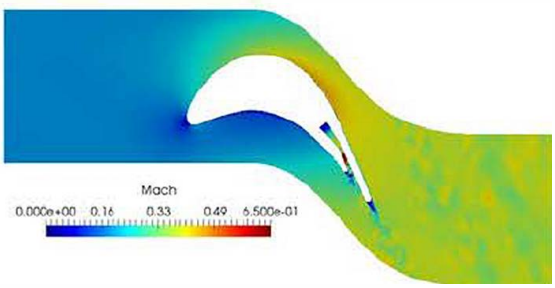

FIGURE 9: SUBSONIC TURBINE BLADE: FINAL STATE.

Following this change of outlet conditions no change is observed, and the final state resulting from it is shown in Fig. 9, depicting a subsonic flow within the inner stator vane channel as targeted.

Turbine blade with choked channel

The maximum mass-flow rate $Q_{ref} = 0.16\ kg/s$ within the vane is targeted in this subsection to evaluate the proposed methodology in the case of supersonic configuration. The same inlet boundary conditions and initial field as previously described are considered here, the outlet static pressure is updated every $T_{update} = 12.5 * 10^{-5}\ s$ while $K = 2.0 * 10^5\ (m.s)^{-1}$. The mass-flow rate temporal evolution of this specific simulation is reported in Fig. 10, showing that the target value is actually reached at $t = 0.06$ s about. However, turning our attention to the outlet static pressure evolution in Fig. 11, it can be shown that a plateau is still not reached at that time. Following instant $t = 0.0077\ s$, several tests are performed modifying T_{update} and K to evaluate their impact on the final state, and show that several final states are likely to occur depending on these parameters.

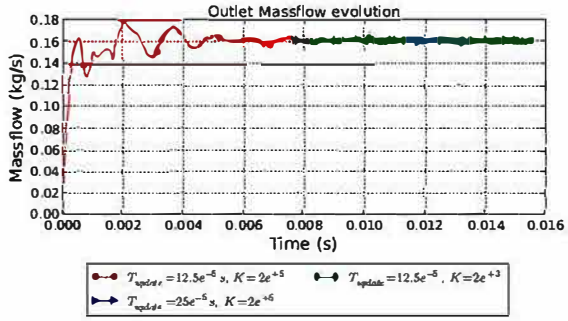

FIGURE 10: CHOKED TURBINE BLADE PASSAGE: MASS-FLOW EVOLUTION.

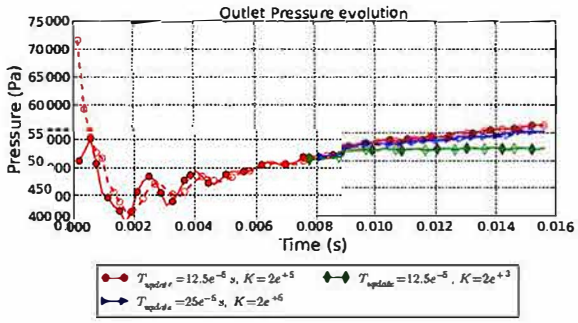

FIGURE 11: CHOKED TURBINE BLADE PASSAGE: OUTLET PRESSURE EVOLUTION. DASHED LINES: PRESCRIPTION, FULL LINES: ACTUAL PRESSURE.

For comparison, the instantaneous Mach number at $t = 0.0077\ s$ is shown in Fig.12, where a contour of $M = 1$ is drawn in black. The inner vane is seen to be adapted as expected, inducing a mass-flow rate independent of the outlet specified pressure. As expected for supersonic outlet conditions, the proposed relaxation method becomes inappropriate and the outlet static pressure must be known in advance.

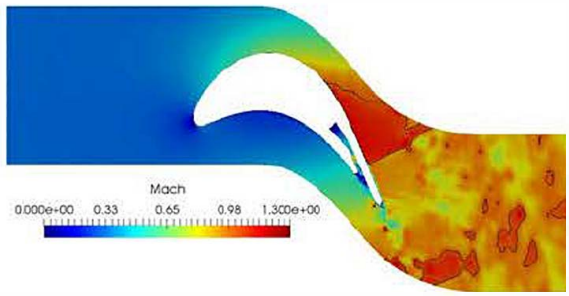

FIGURE 12: CHOKED TURBINE BLADE PASSAGE: INSTANTANEOUS SOLUTION AT $t = 0.0077s$.

Rotor-stator configuration

The proposed overall methodology is finally tested on a 3D rotor-stator configuration representative of an actual industrial problem where the inlet conditions, the rotational speed and the mass-flow rate are known, while the outlet pressure is unknown. The transient from initial state where $N_{fan} = 0$ rpm to the operating point where $N_{fan} = 11614$ rpm is considered in this subsection, which is a delicate part of the simulation, especially for compressors where a small modification of the outlet pressure may significantly modify the operating point. The configuration under study is the fan belonging to the DGEN-380 designed by Price Induction, that is a small turbofan of a small private jet engine. The fan has a bypass ratio of 6, is composed of 14 rotor blades and 40 stator vanes, and has a diameter of 352 mm. More details about the geometry and the operating points may be found in García Rosa et *al.* [49]. To alleviate the computational cost, the numerical domain has been modified to simulate 42 stator vanes, thus ensuring a 360/14° periodicity. The stator chord has been scaled to preserve the original solidity (Rai and Madavan [50]). The mesh considered in this study is a coarse mesh consisting of 50 millions cells. Wall-laws are used to model the boundary layers. More details about the numerical predictions of the average flow and turbulence characteristics on this configu-

ration using the MISCOG methodology may be found in Odier et *al*. [30, 51]. At the inlet, the proposed characteristic formulation is used imposing $P_t = 98803$ Pa, $T_t = 281$ K, and a normal flow direction, while $Q_{ref} = 0.8428$ kg/s is targeted at the outlet. Note that for the entire engine, the total mass-flow rate is $Q = 14 * 0.8428 = 11.8$ kg/s. At the inlet, the experimental turbulence intensity is less than 1%. For this reason, no turbulence is injected in the simulation. The configuration under study is presented in Fig. 13, together with the inlet and outlet boundary condition locations.

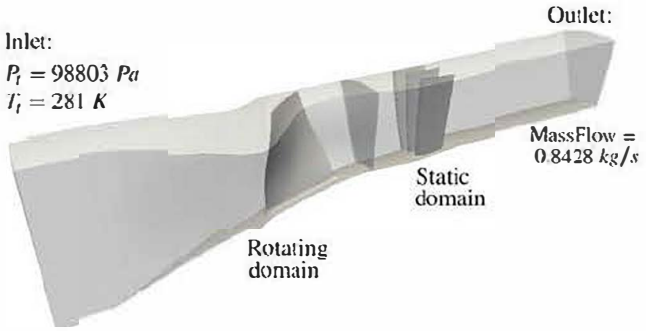

FIGURE 13: ROTOR-STATOR CONFIGURATION: DGEN-380. INLET AND OUTLET BOUNDARY CONDITIONS, AND RESPECTIVE PRESCRIPTIONS.

The outlet relaxation methodology is not considered to start the engine and a fixed static pressure of $P_s = 100000\ Pa$ is arbitrarily imposed at the outlet for the first rotation. Tests have shown that starting the simulation from $N_{fan} = 0$ rpm to $N_{fan} = 11614$ rpm with the proposed relaxation methodology is not adequate, since significant transients occur and a shock is likely to occur in the stator vane resutlting in an inappropriate functionning of the proposition as discussed previously. The proposed relaxation methodology is only considered after an entire rotation, when the flow is established to some arbitrary working point. Note that another methodology may be to initialize the simulation with a first RANS solution. Following this initial state, the temporal evolution of the outlet pressure and mass-flow rate through the outlet boundary are respectively depicted in Figs. 14 and 15, together with the relaxation coefficient K used along the simulation.

Large relaxation coefficients are first considered to rapidly modify the working point and reduce CPU cost. This results in a rapid mass-flow rate convergence to the target value, as shown in Fig. 15 between rotation n°1 and rotation°2. However, it should be noted that the mass-flow rate evolution should not be the only convergence indicator, and that paying attention to the outlet

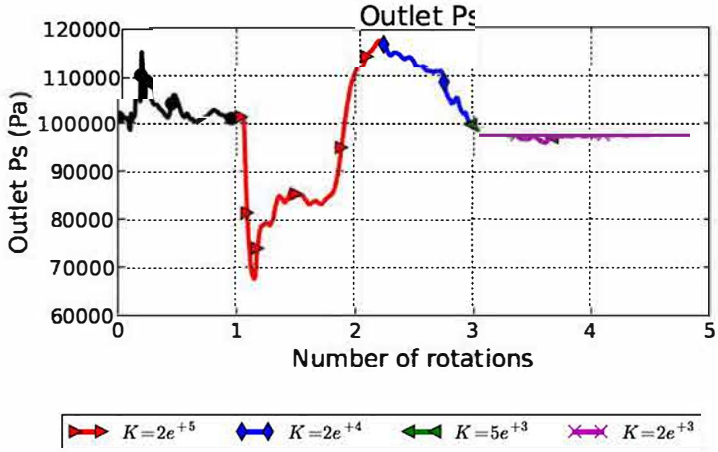

FIGURE 14: ROTOR-STATOR CONFIGURATION: OUTLET STATIC PRESSURE EVOLUTION

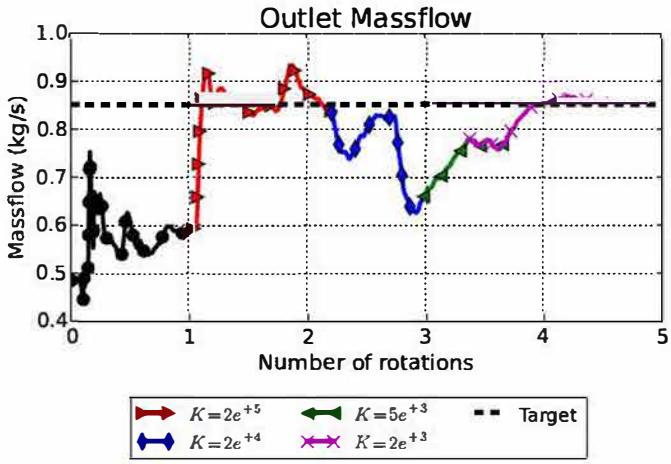

FIGURE 15: ROTOR-STATOR CONFIGURATION: OUTLET MASS-FLOW EVOLUTION

static pressure is mandatory to ensure global convergence. Once the outlet mass-flow rate has reached a value close to the target, the relaxation coefficient K may be progressively decreased. If K is not decreased, the prescribed outlet pressure is likely to experience oscillations, and a reduce in K allows a smooth convergence to the target. At rotation n°4, Fig. 14 shows that the outlet static pressure has nearly reached a converged value, and a constant static pressure $P_s = 98000\ Pa$ is finally imposed. As shown in Fig. 15, this pressure allows the establishement of the mass-flow rate reaching the final target state. The total computational cost for these 4.5 rotations is 14000 hCPU using 360 MPI processes.

CONCLUSION

Inlet and outlet boundary conditions for compressible and unsteady turbomachinery simulations have been addressed in this paper for its use in an industrial context. A characteristic formulation to impose inlet total pressure, total temperature and flow direction is first presented. A relaxation methodology to automatically adjust the outlet static pressure is then presented and evalutated on a turbine blade configuration. A full rotor-stator configuration is finally studied, taking into account the initialisation phase. A best-practise guideline is proposed to users in order to deal with the relaxation coefficients both for the inlet and the outlet boundary conditions.

ACKNOWLEDGMENT

Dr Pierre Aillaud is acknowledged for sharing his turbine blade configuration and for preliminary code implementation. Dr Nicolás García Rosa and Adrien Thacker from ISAE-Supaero, as well as Price Induction are acknowledged for fruitfull discussions and support regarding the DGEN-380 configuration. The computational resources were provided by the GENCI network, and were part of the allocation no. A0032B10157 (CINES-OCCIGEN).

REFERENCES

[1] Scillitoe, A. D., Tucker, P. G., and Adami, P., 2017. "Numerical Investigation of Three-Dimensional Separation in an Axial Flow Compressor : The Influence of Freestream Turbulence Intensity and Endwall Boundary Layer State". *Journal of Turbomachinery,* ***139***(February), pp. 1–10.

[2] Leggett, J., Priebe, S., Shabbir, A., Michelassi, V., Sandberg, R., and Richardson, E., 2018. "Loss Prediction in an Axial Compressor Cascade at Off-Design Incidences With Free Stream Disturbances Using Large Eddy Simulation". *Journal of Turbomachinery,* ***140***(7), p. 071005.

[3] Pogorelov, A., Meinke, M., and Schröder, W., 2015. "Cut-cell method based large-eddy simulation of tip-leakage flow Cut-cell method based large-eddy simulation of tip-leakage flow". *Physics of Fluids,* ***075106***(27), pp. 4–20.

[4] Tyacke, J., Naqavi, I., Wang, Z.-N., Tucker, P., and Boehning, P., 2017. "Predictive Large Eddy Simulation for Jet AeroacousticsCurrent Approach and Industrial Application". *Journal of Turbomachinery,* ***139***(8), p. 081003.

[5] Salas, P., and Moreau, S., 2017. "Aeroacoustic Simulations of a Simplified High-Lift Device Accounting for Some Installation Effects". *AIAA Journal,* ***55***(3), pp. 1–16.

[6] Collado Morata, E., Gourdain, N., Duchaine, F., and Gicquel, L. Y., 2012. "Effects of free-stream turbulence on high pressure turbine blade heat transfer predicted by structured and unstructured les". *International Journal of Heat and Mass Transfer,* ***55***(21-22), pp. 5754–5768.

[7] Dufour, G., Gourdain, N., Duchaine, F., Vermorel, O., and Poinsot, T., 2009. "Numerical Investigations in Turbomachinery : A State of the Art Large Eddy Simulation Applications". In VKI Lecture Series, Von Karman Institute, pp. 21–25.

[8] Gourdain, N., Sicot, F., Duchaine, F., and Gicquel, L., 2014. "Large eddy simulation of flows in industrial compressors: a path from 2015 to 2035". *Philosophical Transactions of the Royal Society A: Mathematical, Physical and Engineering Sciences,* ***372***(2022), pp. 20130323–20130323.

[9] Tucker, P. G., 2011. "Progress in Aerospace Sciences Computation of unsteady turbomachinery flows : Part 1 Progress and challenges". *Progress in Aerospace Sciences,* ***47***(7), pp. 522–545.

[10] Tucker, P. G., 2011. "Progress in Aerospace Sciences Computation of unsteady turbomachinery flows : Part 2 LES and hybrids". *Progress in Aerospace Sciences,* ***47***(7), pp. 546–569.

[11] Tucker, P. G., 2013. *Unsteady Computational Fluid Dynamics in Aeronautics*. Springer.

[12] Segui, L. M., Gicquel, L. Y. M., Duchaine, F., and Laborderie, J. D., 2018. "Importance of boundary layer transition in a high-pressure turbine cascade using LES". In ASME Turbo Expo 2018: Turbomachinery Technical Conference & Exposition, pp. 1–10.

[13] Sayadi, T., and Moin, P., 2012. "Large eddy simulation of controlled transition to turbulence". *Physics of Fluids,* ***24***(11).

[14] Spalart, P. R., Jou, W.-H., Strelets, M. L., and Allmaras, S. R., 1997. "Comments on the feasibility of LES for wings, and on a hybrid RANS/LES approach". In Proceedings of the First AFOSR International Conference on DNS/LES.

[15] Deck, S., 2005. "Zonal-Detached-Eddy Simulation of the Flow Around a High-Lift Configuration". *AIAA Journal,* ***43***(11), pp. 2372–2384.

[16] Boudet, J., Cahuzac, A., Kausche, P., and Jacob, M., 2015. "Zonal Large-Eddy Simulation of a Fan Tip-Clearance Flow, With Evidence of Vortex Wandering". *Journal of Turbomachinery,* ***137***(6), p. 061001.

[17] Bose, S. T., and Park, G. I., 2018. "Wall-Modeled Large-Eddy Simulation for Complex Turbulent Flows". *Annual Review of Fluid Mechanics,* ***50***(1), pp. 535–561.

[18] Larsson, J., and Wang, Q., 2014. "The prospect of using large eddy and detached eddy simulations in engineering design, and the research required to get there". *Philosophical Transactions of the Royal Society A: Mathematical, Physical and Engineering Sciences,* ***372***(2022), pp. 1–15.

[19] Odier, N., Sanjosé, M., Gicquel, L., Poinsot, T., Moreau, S., and Duchaine, F., 2019. "A characteristic inlet boundary condition for compressible, turbulent, multispecies turbo-

machinery flows". *Computers & Fluids,* ***178***, jan, pp. 41–55.

[20] Schønfeld, T., and Rudgyard, M., 1999. "Steady and unsteady flows simulations using the hybrid flow solver avbp". *AIAA Journal,* ***37***, pp. 1378–1385.

[21] Gourdain, N., Gicquel, L., Montagnac, M., Vermorel, O., Gazaix, M., Staffelbach, G., Garcia, M., Boussuge, J.-F., and Poinsot, T., 2009. "High performance parallel computing of flows in complex geometries: I. Methods". *Computational Science & Discovery,* ***2***(1), p. 015003.

[22] Lax, P., and Wendroff, B., 1960. "Systems of conservation laws". *Commun. Pure Appl. Math,* ***13***(2), pp. 217–237.

[23] Colin, O., and Rudgyard, M., 2000. "Development of High-Order TaylorGalerkin Schemes for LES". *Journal of Computational Physics,* ***162***(2), pp. 338–371.

[24] Wang, G., Duchaine, F., Papadogiannis, D., Duran, I., Moreau, S., and Gicquel, L., 2014. "An overset grid method for large eddy simulation of turbomachinery stages". *Journal of Computational Physics,* ***274***, pp. 333–355.

[25] de Laborderie, J., Duchaine, F., Gicquel, L., Vermorel, O., Wang, G., and Moreau, S., 2018. "Numerical analysis of a high-order unstructured overset grid method for compressible LES of turbomachinery". *Journal of Computational Physics,* ***363***, pp. 371–398.

[26] De Laborderie, J., Duchaine, F., Vermorel, O., Gicquel, L., and Moreau, S., 2016. "Application of an overset grid method to the large eddy simulation of a high-speed multi-stage axial compressor". In ASME Turbo Expo, GT2016-56344.

[27] Dombard, J., Duchaine, F., Gicquel, L., Staffelbach, G., Buffaz, N., and Trébinjac, I., 2018. "Large Eddy Simulations in a Transonic Centrifugal Compressor". In ASME Turbo Expo 2018: Turbomachinery Technical Conference & Exposition, pp. 1–10.

[28] Wang, G., Moreau, S., de Laborderie, J., and Gicquel, L. Y. M., 2014. "LES Investigation of Aerodynamics Performance in an Axial Compressor Stage LES Investigation of Aerodynamics Performance in an Axial Compressor Stage". In 22nd Annual Conference of the CFD Society of Canada, no. June.

[29] Leonard, T., Sanjose, M., Moreau, S., and Duchaine, F., 2016. "Large Eddy Simulation of a scale-model turbofan for fan noise source diagnostic". In 22nd AIAA/CEAS Aeroacoustics Conference, 2016-3000.

[30] Odier, N., Thacker, A., Duchaine, F., Gicquel, L., Staffelbach, G., García Rosa, N., Dufour, G., and Mueller, J.-D., 2018. "Evaluation of Integral Turbulence Scale Through the Fan Stage of A Turbofan Using Hot Wire Anemometry and Large Eddy Simulation". In ASME Turbo Expo 2018: Turbomachinery Technical Conference & Exposition, pp. 1–13.

[31] Pérez Arroyo, C., Leonard, T., Sanjosé, M., Moreau, S., and Duchaine, F., 2017. "Large Eddy Simulation of a Scale-model Turbofan for Fan Noise Source Large Eddy Simulation of a Scale-model Turbofan for Fan Noise Source Diagnostic". In International Symposium on Trnasport Phenomena and Dynamics of Rotating Machinery, no. December, pp. 1–12.

[32] Duchaine, F., Dombard, J., Gicquel, L. Y., and Koupper, C., 2017. "On the importance of inlet boundary conditions for aerothermal predictions of turbine stages with large eddy simulation". *Computers and Fluids,* ***154***, pp. 60–73.

[33] Papadogiannis, D., Wang, G., Moreau, S., Duchaine, F., Gicquel, L., and Nicoud, F., 2015. "Assessment of the Indirect Combustion Noise Generated in a Transonic High-Pressure Turbine Stage". *Journal of Engineering for Gas Turbines and Power,* ***138***(4), p. 041503.

[34] Wang, G., Sanjose, M., Moreau, S., Papadogiannis, D., Duchaine, F., and Gicquel, L., 2016. "Noise mechanisms in a transonic high-pressure turbine stage". *International Journal of Aeroacoustics,* ***15***, pp. 1–18.

[35] Thompson, K. W., 1987. "Time dependent boundary conditions for hyperbolic systems". *Journal of Computational Physics,* ***68***(1), pp. 1–24.

[36] Poinsot, T. J., and Lele, S. K., 1992. "Boundary conditions for direct simulations of compressible viscous flows". *Journal of Computational Physics,* ***101***(1), pp. 104–129.

[37] Rudy, H., and Strikwerda, J. C., 1980. "A nonreflecting outflow boundary condition for subsonic Navier-Stokes calculations". *Journal of Computational Physics,* ***36***, pp. 55–70.

[38] Kraichnan, R. H., 1970. "Diffusion by a Random Velocity Field". *Physics of Fluids,* ***13***(1), p. 22.

[39] Smirnov, A., Shi, S., and Celik, I., 2001. "Random Flow Generation Technique for Large Eddy Simulations and Particle-Dynamics Modeling". *Journal of Fluids Engineering,* ***123***(2), p. 359.

[40] Passot, T., and Pouquet, A., 1987. "Numerical simulation of compressible homogeneous flows in the turbulent regime". *Journal of Fluid Mechanics,* ***181***(-1), p. 441.

[41] Guézennec, N., and Poinsot, T., 2009. "Acoustically Nonreflecting and Reflecting Boundary Conditions for Vorticity Injection in Compressible Solvers". *AIAA Journal,* ***47***(7), pp. 1709–1722.

[42] Lodato, G., Domingo, P., and Vervisch, L., 2008. "Three-dimensional boundary conditions for direct and large-eddy simulation of compressible viscous flows". *Journal of Computational Physics,* ***227***(10), pp. 5105–5143.

[43] Granet, V., Vermorel, O., Léonard, T., Gicquel, L., and Poinsot, T., 2010. "Comparison of Nonreflecting Outlet Boundary Conditions for Compressible Solvers on Unstructured Grids". *AIAA Journal,* ***48***(10), pp. 2348–2364.

[44] Koupper, C., Poinsot, T., Gicquel, L. Y. M., and Duchaine, F., 2014. "Compatibility of Characteristic Boundary Conditions with Radial Equilibrium in Turbomachinery Simu-

lations". *AIAA Journal,* ***52***(12), pp. 2829–2839.

[45] De Laborderie, J., Duchaine, F., and Gicquel, L., 2017. "Analysis of a high-pressure multistage axial compressor at off-design conditions with coarse large eddy simulations". In 12th European Conference on Turbomachinery Fluid Dynamics and Thermodynamics, ETC 2017, pp. 1–13.

[46] Aillaud, P., Duchaine, F., Gicquel, L. Y. M., and Koupper, C., 2018. "on the Use of Periodic Boundary Condition for Large Eddy Simulation of Trailing Edge Cutback Film Cooling With Internal Ribs". In ASME Turbo Expo 2018, pp. 1–12.

[47] Rehder, H.-J., 2006. Design, manufacture and instrumentation of cascade and cooling blades at dlr (european research project aiteb-2). Tech. rep., Dezember.

[48] Rehder, H.-J., 2012. "Investigation of Trailing Edge Cooling Concepts in a High Pressure Turbine CascadeAerodynamic Experiments and Loss Analysis". *Journal of Turbomachinery,* ***134***(5), p. 051029.

[49] García Rosa, N., Dufour, G., Barènes, R., and Lavergne, G., 2015. "Experimental Analysis of the Global Performance and the Flow Through a High-Bypass Turbofan in Windmilling Conditions". *Journal of Turbomachinery,* ***137***(5), p. 051001.

[50] Rai, M., and Madavan, N. K., 1990. "Multi-Airfoil Navier-Stokes Simulations of Turbine Rotor-Stator Interaction". *Journal of Turbomachinery,* ***112***(July), pp. 377–384.

[51] Odier, N., Duchaine, F., Gicquel, L., Dufour, G., and García Rosa, N., 2017. "Comparison of LES and RANS predictions with experimental results of the fan of a turbofan". In 12th European Turbomachinery Conference, pp. 1–14.